

2019

## Investigating risk factors and predicting complications in deep brain stimulation surgery with machine learning algorithms

Farrokh Farrokhi

Quinlan D. Buchlak

Matt Sikora

Nazanin Esmaili

Maria Marsans

*See next page for additional authors*

Follow this and additional works at: [https://researchonline.nd.edu.au/med\\_article](https://researchonline.nd.edu.au/med_article)



This article was originally published as:

Farrokhi, F., Buchlak, Q. D., Sikora, M., Esmaili, N., Marsans, M., McLeod, P., Mark, J., Cox, E., Bennett, C., & Carlson, J. (2019). Investigating risk factors and predicting complications in deep brain stimulation surgery with machine learning algorithms. *World Neurosurgery, Early View, Online First*.

Original article available here:

<https://doi.org/10.1016/j.wneu.2019.10.063>

This article is posted on ResearchOnline@ND at [https://researchonline.nd.edu.au/med\\_article/1090](https://researchonline.nd.edu.au/med_article/1090). For more information, please contact [researchonline@nd.edu.au](mailto:researchonline@nd.edu.au).



---

**Authors**

Farrokh Farrokhi, Quinlan D. Buchlak, Matt Sikora, Nazanin Esmaili, Maria Marsans, Pamela McLeod, Jamie Mark, Emily Cox, Christine Bennett, and Jonathan Carlson



©2019

This manuscript version is made available under the CC-BY-NC-ND 4.0 International license <http://creativecommons.org/licenses/by-nc-nd/4.0/>

This is the accepted manuscript version of an article published as:

Farrokhi, F., Buchlak, Q.D., Sikora, M., Esmaili, N., Marsans, M., McLeod, P., Mark, J., Cox, E., Bennett, C., and Carlson, J. (2019). Investigating risk factors and predicting complications in deep brain stimulation surgery with machine learning algorithms. *World Neurosurgery, Online First*. doi: 10.1016/j.parint.2019.101993

This article has been published in final form at <https://doi.org/10.1016/j.parint.2019.101993>

# Journal Pre-proof

Investigating risk factors and predicting complications in deep brain stimulation surgery with machine learning algorithms

Farrokh Farrokhi, MD, Quinlan D. Buchlak, MPsy MBIS, Matt Sikora, BA, Nazanin Esmaili, PhD, Maria Marsans, PAC, Pamela McLeod, PAC, Jamie Mark, ARNP, Emily Cox, PhD, Christine Bennett, MBBS, Jonathan Carlson, MD PhD

PII: S1878-8750(19)32681-6

DOI: <https://doi.org/10.1016/j.wneu.2019.10.063>

Reference: WNEU 13534

To appear in: *World Neurosurgery*

Received Date: 6 July 2019

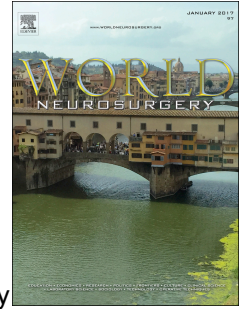
Revised Date: 9 October 2019

Accepted Date: 10 October 2019

Please cite this article as: Farrokhi F, Buchlak QD, Sikora M, Esmaili N, Marsans M, McLeod P, Mark J, Cox E, Bennett C, Carlson J, Investigating risk factors and predicting complications in deep brain stimulation surgery with machine learning algorithms, *World Neurosurgery* (2019), doi: <https://doi.org/10.1016/j.wneu.2019.10.063>.

This is a PDF file of an article that has undergone enhancements after acceptance, such as the addition of a cover page and metadata, and formatting for readability, but it is not yet the definitive version of record. This version will undergo additional copyediting, typesetting and review before it is published in its final form, but we are providing this version to give early visibility of the article. Please note that, during the production process, errors may be discovered which could affect the content, and all legal disclaimers that apply to the journal pertain.

© 2019 Elsevier Inc. All rights reserved.



# Investigating risk factors and predicting complications in deep brain stimulation surgery with machine learning algorithms

Farrokh Farrokhi MD<sup>1</sup>, Quinlan D. Buchlak MPsy MBIS<sup>2</sup>, Matt Sikora BA<sup>1</sup>, Nazanin Esmaili PhD<sup>2,3,4</sup>, Maria Marsans PAC<sup>1</sup>, Pamela McLeod PAC<sup>5</sup>, Jamie Mark ARNP<sup>6</sup>, Emily Cox PhD<sup>7</sup>, Christine Bennett MBBS<sup>2</sup>, Jonathan Carlson MD PhD<sup>5</sup>

<sup>1</sup>Neuroscience Institute, Virginia Mason Medical Center, Seattle, WA, USA

<sup>2</sup>School of Medicine, University of Notre Dame Australia, Sydney, NSW, Australia

<sup>3</sup>Department of Medicine, University of Toronto, Toronto, ON, Canada

<sup>4</sup>Faculty of Engineering and IT, University of Technology Sydney, Ultimo, NSW, Australia

<sup>5</sup>Inland Neurosurgery and Spine Associates, Spokane, WA, USA

<sup>6</sup>Selkirk Neurology, Spokane, WA, USA

<sup>7</sup>Providence Medical Research Center, Providence Health & Services, Spokane, WA, USA

## Corresponding author:

Quinlan Buchlak

The University of Notre Dame

160 Oxford St

Sydney, Australia, 2015

E-mail: quinlan.buchlak1@my.nd.edu.au

**Element counts:** Abstract word count = 248; text word count (excluding abstract) = 4191; number of references = 87; number of tables = 5; number of figures = 4.

**Disclosures:** All authors have reviewed and approved this manuscript and have no relevant financial or other conflicts of interest with regard to this research and its publication.

**Keywords:** Risk stratification, data imputation, machine learning, supervised learning, gradient boosting machines, deep brain stimulation, neurosurgery

1 **ABSTRACT**

2 **Background:** Deep brain stimulation (DBS) surgery is an option for patients experiencing  
3 medically resistant neurological symptoms. DBS complications are rare; finding significant predictors  
4 requires a large number of surgeries. Machine learning algorithms may be used to effectively predict  
5 these outcomes. The aims of this study were to (1) investigate preoperative clinical risk factors, and (2)  
6 build machine learning models to predict adverse outcomes.

7 **Methods:** This multicenter registry collected clinical and demographic characteristics of patients  
8 undergoing DBS surgery (n=501) and tabulated occurrence of complications. Logistic regression was  
9 used to evaluate risk factors. Supervised learning algorithms were trained and validated on 70% and  
10 30%, respectively, of both oversampled and original registry data. Performance was evaluated using  
11 area under the receiver operating characteristics curve (AUC), sensitivity, specificity and accuracy.

12 **Results:** Logistic regression showed that the risk of complication was related to the operating  
13 institution in which the surgery was performed (OR=0.44, confidence interval [CI]=0.25-0.78), BMI  
14 (OR=0.94,CI=0.89-0.99) and diabetes (OR=2.33,CI=1.18-4.60). Patients with diabetes were almost  
15 three times more likely to return to the operating room (OR=2.78,CI=1.31-5.88). Patients with a history  
16 of smoking were four times more likely to experience postoperative infection (OR=4.20,CI=1.21-  
17 14.61). Supervised learning algorithms demonstrated high discrimination performance when predicting  
18 any complication (AUC=0.86), a complication within 12 months (AUC=0.91), return to the operating  
19 room (AUC=0.88) and infection (AUC=0.97). Age, BMI, procedure side, gender and a diagnosis of  
20 Parkinson's disease were influential features.

21 **Conclusions:** Multiple significant complication risk factors were identified and supervised learning  
22 algorithms effectively predicted adverse outcomes in DBS surgery.

23

## 24 INTRODUCTION

25 The primary aim of this study was to look at which preoperative clinical factors were related to  
26 complications that develop in deep brain stimulation (DBS) therapy. DBS is a safe, effective and  
27 common surgical intervention for a range of neurological disorders including Parkinson's disease and  
28 essential tremor<sup>1-7</sup>. Through electrodes implanted in the brain, DBS therapy stimulates deep subcortical  
29 brain structures, including the subthalamic nucleus (STN), the ventral intermedius nucleus (VIM) and  
30 the globus pallidus (GPi) to alleviate neurological symptoms like tremor, motor fluctuations, and  
31 rigidity<sup>4,5,8</sup>. It is a treatment modality that is considered when a patient's symptoms have not been  
32 satisfactorily alleviated by medical management<sup>9-14</sup>.

33 DBS therapy requires an initial electrode implantation operation and subsequent surgery to place  
34 device generators. Potential complications arising from DBS surgery include infection, intracerebral  
35 hemorrhage, seizures and hardware failure, which can lead to unplanned return to the operating room.  
36 Post-operative readmission rates range from 1.9% (30-day) to 4.3% (90-day)<sup>1</sup>. Factors likely associated  
37 with complications include age, smoking history, obesity, diabetes, hypertension and facility surgical  
38 volume<sup>1,15</sup>. Advanced age and hypertension have been associated with the risk of intracranial  
39 hemorrhage<sup>16</sup>, and readmission after DBS surgery has been associated with preoperative coronary  
40 artery disease, obesity and a history of smoking<sup>1</sup>. Further, there is a seasonal variation in DBS  
41 infection, often referred to as the July effect<sup>17</sup>.

42 Integrating preoperative risk assessment into standard clinical care fosters a shared decision making  
43 process between the surgical team, the patient and clinical enablers<sup>18</sup>. Performing pre-operative risk  
44 assessment for DBS procedures is challenging due to limited data suggesting the contributions of  
45 individual risk factors to post-operative complications. It is arguable that the literature surrounding  
46 DBS surgery risk remains inconclusive because the low frequency of complications limits the power  
47 and sensitivity of traditional statistical methods. To study this problem, a multi-institutional database of  
48 complications and risk factors was compiled, and a pilot study analysed it. Similar to the literature, the  
49 only relationship found was an association between smoking and infection risk. The standard statistical  
50 methods applied were ineffective at determining significant clinical risk factors related to  
51 complications, such as body mass index, diabetes, hypertension, smoking, and age. So, a different

52 approach to identifying relationships between complications and risk factors, involving the use of  
53 machine learning, was designed and deployed.

54 Machine learning, a branch of artificial intelligence, represents a powerful set of technologies that  
55 enable three main tasks: classification, regression and clustering <sup>19</sup>. Supervised learning involves  
56 training algorithms with datasets that contain labelled outcomes for each case. Supervised learning (i.e.,  
57 classification and regression) uses input features (X) to predict a defined outcome (Y), while  
58 unsupervised learning (i.e., clustering) involves analyzing input variables (X) to elucidate patterns and  
59 structure in the data. Supervised learning algorithms can predict rare events such as surgical  
60 complications <sup>20</sup> and have the potential to improve patient risk stratification, clinical decision making,  
61 informed consent and health service planning <sup>18,21-25</sup>. Supervised learning has been used in DBS surgery  
62 to predict clinical outcomes <sup>26,27</sup>, surgical targets <sup>28,29</sup>, side effects <sup>30</sup>, discharge status <sup>31</sup> and  
63 neurophysiological detection of DBS structures <sup>32-34</sup>.

64 Extreme gradient boosting machines (XGBM) are a type of supervised learning algorithm. It uses  
65 decision tree-based learning and shows strong performance on a diverse array of problems. It operates  
66 by strategically combining networks of sequential decision trees. Later decision tree models correct  
67 inaccuracies in previous models to improve prediction performance <sup>35</sup>. An XGBM model is comprised  
68 of an ensemble of decision trees. The development of algorithms that incorporate gradient boosting has  
69 produced highly robust regression and classification methods <sup>36</sup>. XGBMs appear to have performed  
70 well in various domains <sup>35,37-41</sup> and have been shown to perform particularly well on datasets  
71 characterized by class imbalance <sup>42,43</sup>. Many supervised learning algorithms perform well as predictive  
72 tools partly because they can estimate complex nonlinear relationships in high volume datasets using  
73 weighted statistical functions in a way that cannot be perceived by linear models or clinicians <sup>44-47</sup>.  
74 Logistic regression is one such linear classification model. Two advantages it affords are that it is easily  
75 interpretable, and it delivers measures of statistical significance.

76 Class imbalance describes a situation where the number of one event type (e.g., postoperative DBS  
77 complications) is very low compared to another event type (e.g., no postoperative DBS complications)  
78 <sup>48</sup>. A class is a subcategory within a variable in a dataset. For example, within a variable capturing data  
79 on postoperative complications, one class may represent the complication state, while another class may



80 represent the no-complication state. Class imbalance essentially refers to differences in class  
81 probabilities<sup>49</sup>. Postoperative DBS complications are low probability events. There is a much higher  
82 probability that DBS patients will experience no postoperative complications. This imbalanced outcome  
83 probability is what is meant by researchers referring to imbalanced classes. Chawla (2010) states that a  
84 dataset is imbalanced if the classification categories are not equally represented<sup>50</sup>. The performance of  
85 some supervised learning algorithms is undermined by class imbalance, resulting in output  
86 classifications that default simply to the majority class<sup>51-53</sup>. However, class imbalance characterizes  
87 many real-world datasets from biomedicine<sup>52</sup>, to finance<sup>54</sup>, aviation<sup>55</sup> and geoscience<sup>56</sup>. Class  
88 imbalance is one of the main barriers to effectively predicting postoperative complications in  
89 neurosurgery<sup>18,19,24,31</sup>.

90 Because the class imbalance problem is so prevalent<sup>53</sup>, much research in the fields of predictive  
91 analytics, data mining and machine learning has focused on developing and testing methods to  
92 effectively address it, at both the algorithm and data levels<sup>49,51,52,57-59</sup>. The Synthetic Minority  
93 Oversampling Technique (SMOTE) has emerged as one effective method of addressing the class  
94 imbalance issue at the data level<sup>59</sup>. It operates by creating additional synthetic cases based upon  
95 existing minority cases and the k-nearest neighbor algorithm. It balances the class distribution by  
96 synthesizing new additional minority class examples through a process of interpolating between  
97 multiple minority class examples that lie together in multidimensional space. In this way, SMOTE has  
98 been intentionally designed to avoid the predictive analytics problem of overfitting<sup>53</sup>. Another strength  
99 of employing the SMOTE method is that no cases in the dataset need to be excluded from the predictive  
100 analysis, which is particularly useful in neurosurgery where cases are not common and datasets are  
101 often not large (i.e., hundreds of cases rather than thousands). The application of SMOTE may  
102 effectively facilitate the prediction of DBS complications, which would be of substantial utility to  
103 clinicians.

104 This study sought to answer the following two research questions. Can multivariate logistic  
105 regression detect significant associations between preoperative variables and postoperative outcomes?  
106 Can DBS complications be accurately predicted by applying the XGBM algorithm and SMOTE?

**107 METHOD****108 Subjects**

109 This study was approved by Institutional Review Boards at each study site. Due to the retrospective  
110 nature of the study, the requirement for informed consent was waived. A combined registry was created  
111 comprising 501 adults who underwent initial DBS implantation surgeries between October 1997 and  
112 May 2018 at two private practices. Procedures included were performed by five neurosurgeons at two  
113 neurosurgical centers over a 22-year period. Patients underwent DBS implantation for Parkinson's  
114 disease (n=348), essential tremor (n=129), dystonia (n=11) and other indications (n=13).

**115 Surgical Technique**

116 The general surgical technique was relatively similar among all surgeons. Primary surgeons at each  
117 institution each had >15 years of experience in DBS surgery. A frame-based approach was used in  
118 patients with DBS lead placement (unilateral or bilateral) using Medtronic 3389 or 3379 leads.  
119 Microelectrode recording was used in all cases. A single microelectrode was used to identify and  
120 confirm the target in all cases. The average number of microelectrode passes per lead was 1.4.  
121 Intraoperative imaging of lead location with cone beam CT was performed in some cases beginning in  
122 2008. The majority of patients underwent intraoperative bipolar review of clinical efficacy and side  
123 effects in an "awake" state<sup>60</sup>. Generator placement was staged one to two weeks after initial lead  
124 implantation. All patients underwent postoperative MRI and/or CT scans within a week of lead  
125 implantation.

**126 Data**

127 Pre-existing quality assurance databases of DBS patients and their outcomes from both research  
128 sites were combined. Additional retrospective data were collected from electronic medical records.  
129 Potential risk factors were recorded, including age, gender, BMI, clinical diagnosis, smoking history,  
130 immunosuppression, hypertension (medications taken within 90 days of surgery), diagnosis of diabetes  
131 mellitus, hypertension, surgical target (VIM, STN, GPi) and procedure side (left, right, bilateral).

132 Complication categories were intracranial hemorrhage, readmission, ischemic infarction, seizure,  
133 lead fracture, electrode migration, loose or flipping battery needing surgical revision, device

134 malfunction, return to the operating room and infection. An infection was defined as an event requiring  
135 surgical removal of hardware, regardless of the time after implantation. This included perioperative  
136 infections within 3 months of surgery, as well as delayed infection associated with hardware erosion or  
137 other systemic infections and infections after generator replacement surgery that could have been years  
138 later. Intracranial hemorrhage was defined as any form of new post-operative bleeding on radiology  
139 report, with or without neurological sequelae and not necessarily requiring surgical intervention. Return  
140 to the operating room included all surgeries that required a return to the operating room, regardless of  
141 time since lead implantation, for indications including haemorrhage, infection, erosion of hardware,  
142 fracture of hardware detected on imaging or as open circuit on programming, revision of lead location,  
143 revision of flipping or loose generator, or tight extension wires. Four primary outcomes were recorded  
144 for each patient: any postoperative complication, a complication within 12 months of surgery, return to  
145 the operating room and infection.

#### 146 **Analysis**

147 Unilateral (n=151), simultaneous bilateral (n=296) and staged bilateral lead implantation (n=54)  
148 were counted each as a single case. Descriptive statistics, multivariate logistic regression and  
149 supervised learning model development were performed using Python 3.6.

#### 150 ***Neural network development for BMI data imputation***

151 Missing data can create problems for some supervised learning algorithms and may necessitate  
152 dropping entire cases. Further, missing data can adversely affect the validity of results<sup>61</sup>. Out of 501  
153 cases, there were 51 missing BMI values. Given the scarce nature of DBS case data and the resources  
154 required to collect it, the research team was motivated to retain as many cases as possible for analysis.  
155 Data imputation addresses this issue and various methods can be used<sup>61-65</sup>. Four neural network  
156 regression models were developed to impute BMI for the cases with missing data. BMI values were  
157 imputed using all pre- and post-operative variables in the dataset. One neural network was selected for  
158 imputation regression because it demonstrated the best performance. Mean BMI before and after  
159 imputation did not differ significantly (27.57, SD=5.06 and 27.39, SD=5.98, respectively; p=0.58).

#### 160 ***Feature selection***

161 Three criteria were used when selecting input features for the models: (1) existing evidence in the  
162 literature suggesting a relationship between the feature and the outcome, (2) availability of the feature  
163 in the dataset; and (3) clinical expert approval that the feature under consideration was clinically related  
164 to the outcome variable.

#### 165 ***Multivariate logistic regression to detect associations***

166 Multivariate logistic regression was conducted using the statsmodels [53] and scikitlearn [54]  
167 packages. Multivariate model performance, odds ratios (OR) and confidence intervals (CI) were  
168 calculated for each risk factor. Features with negligible statistical contribution to multivariate models  
169 (z-score <0.02) were excluded and models were subsequently retrained.

#### 170 ***XGBM model development for postoperative complication prediction***

171 Multiple classifiers were tested and compared to predict postoperative complication outcomes,  
172 including logistic regression, random forests, decision trees and support vector machines. Algorithm  
173 performance statistics were compared using multiple metrics including area under the receiver  
174 operating characteristic curve (AUC), accuracy, sensitivity, specificity, positive predictive value and  
175 negative predictive value. XGBM was among the highest performing classifiers. Because of this and  
176 previous literature demonstrating strong performance on imbalanced datasets, multiple XGBM models  
177 were developed using the XGBoost<sup>66</sup> package. For each of the four primary outcome variables, three  
178 XGBM models were created: one using the original dataset, one using the SMOTE dataset<sup>59</sup>, and one  
179 using a SMOTE training dataset with a non-SMOTE validation dataset.

180 Each model was trained on a 70% sample of the dataset and validated on the remaining 30%. In the  
181 original dataset, this resulted in 350 training cases and 151 validation cases. In the SMOTE  
182 oversampled datasets, ratios of training:validation case numbers were as follows: any complication,  
183 585:251; complication within 12 months, 618:266; return to the operating room, 627:269; and infection,  
184 663:285. SMOTE was selected over other techniques to address class imbalance because (1) it allowed  
185 retention and use of all cases in the DBS dataset, (2) it was designed to avoid overfitting, and (3) it has  
186 been implemented as an accessible Python package.

187 Hyperparameter tuning involving grid-search with 5-fold cross-validation was used to find optimal  
188 XGBM parameters. Grid-search employed 1512 hyperparameter combinations, resulting in 7560 fit  
189 cycles for each of the XGBM models. Using the optimal hyperparameters found in the grid-search  
190 process, internal cross-validation was conducted with the number of boosting rounds set at 50 and the  
191 number of early stopping rounds set at 10. AUC was used as the performance metric in this process.

192 Predictions were made using the optimized model and the validation test sets. Confusion matrices  
193 and performance statistics were computed. Performance metrics included AUC, accuracy, sensitivity,  
194 specificity, positive predictive value and negative predictive value <sup>44,67,68</sup>. Feature importance was  
195 calculated, decision trees were visualized and receiver operating characteristics (ROC) curves  
196 developed. Figure 1 outlines the analysis process overall.

197

**198 RESULTS**

199 Descriptive statistics are displayed in Table 1. Mean age at implant was  $64\pm 10.3$  years. The  
200 majority of patients were male (63%), were diagnosed with Parkinson's disease (70%), had a BMI of  
201 25 or more (67%) and underwent a simultaneous bilateral (59%) STN procedure (70%). Patient  
202 characteristics did not differ significantly between institutions.

**203 Complication Rates**

204 There were 27 (5.4%) infections over the period of observation (mean 455 days). These infections  
205 were either perioperative, occurring within 3 months of lead implantation in 13 (2.6%) patients, or  
206 delayed in 14 (2.8%) patients. The median time to onset of all infections was 3.3 months. Delayed  
207 infections were typically related to hardware erosion, systemic infections, generator replacement, or  
208 appeared spontaneously.

209 Surgical revision of hardware occurred in 26 (5.2%) patients, on average 28 months after initial  
210 implantation. These revisions were for lead or extension wire fracture in 18 (3.6%) patients, loose  
211 hardware in seven (1.4%), or repositioned leads due to side effects or poor efficacy in eight (1.6%).

212 Intracranial hemorrhage occurred in 15 (3.0%) patients, all associated with lead implantation. This  
213 included intraparenchymal hemorrhage along the lead and subdural hematoma. No deaths occurred in  
214 any of these cases. Of these hemorrhages, 2 of 501 patients (0.4%) had substantial morbidity requiring  
215 surgical intervention. Other hemorrhages, 13 (2.6%), were observed on imaging, and resolved without  
216 surgical treatment or neurological sequelae.

**217 Risk factors identified using logistic regression**

218 Logistic regression demonstrated statistically significant relationships between risk factors and  
219 complications (Table 2). Diabetic patients were nearly three times more likely to return to the operating  
220 room than those without diabetes (OR=2.78, CI=1.31-5.88,  $p<0.01$ ). Postoperative infection was  
221 associated with a history of smoking (OR=4.20, CI=1.21-14.61,  $p<0.05$ ). It appeared that patients with  
222 a history of smoking were more than four times more likely to experience postoperative infection.  
223 Experiencing any type of complication was associated with operating institution (OR=0.44, CI=0.25-  
224 0.78,  $p<0.01$ ), BMI (OR=0.94, CI=0.89-0.99,  $p<0.05$ ) and diabetes (OR=2.33, CI=1.18-4.60,  $p<0.05$ ).

225 Operating institution was also significantly associated with experiencing a complication within 12  
226 months (OR=0.36, CI=0.18-0.70,  $p<0.01$ ). The institution with slightly higher complication rates  
227 appeared to have operated on a patient sample with higher comorbidity rates (Table 3).

### 228 **Complication prediction with XGBM models**

229 XGBM models coupled with the SMOTE dataset demonstrated strong predictive performance  
230 (Table 4). These models demonstrated higher performance (validation AUC: 0.86-0.97) compared to  
231 models trained and validated on the original dataset (validation AUC: 0.57-0.69). Models based on the  
232 SMOTE dataset predicted high numbers of true positives and true negatives. Models trained on the  
233 SMOTE training dataset and validated on the non-SMOTE holdout sample demonstrated performance  
234 that was not substantially superior to the models trained on the original dataset.

235 ROC curves were generated by running the trained models on the holdout validation datasets. The  
236 ROC curves and corresponding AUC associated with the four SMOTE XGBM models showed strong  
237 performance (Figure 2).

### 238 **Plotting feature importance**

239 Feature importance metrics were plotted for each of the SMOTE XGBM models (Figure 3). Age,  
240 BMI, procedure side, gender, a diagnosis of Parkinson's disease, institution and comorbidities appeared  
241 to be the most influential predictive features associated with complications. Feature importance  
242 appeared to vary slightly by model. When plotting complicated cases in the original dataset according  
243 to BMI and age, cases clustered at approximately age 70 and a BMI of 24 (Figure 4).

### 244 **Carrying out predictions on hypothetical patient data**

245 A set of hypothetical patients is shown to demonstrate the output of the XGBM predictive models  
246 (Table 5). Risk thresholds similar to those developed in cardiology risk stratification research were  
247 applied to facilitate interpretation of model output (low= $<10\%$ , moderate=10-15%, high=16-50%, very  
248 high= $>50\%$ )<sup>69</sup>.

249

250 **DISCUSSION**

251 This study found multiple clinical predictors of complications in DBS surgery using supervised  
252 machine learning algorithms. Logistic regression showed that patient BMI, diabetes and operating  
253 institution were significantly associated with all complications grouped together. Diabetics were almost  
254 three times more likely to return to the operating room. A history of smoking was significantly  
255 associated with postoperative infection.

256 The XGBM supervised learning algorithm demonstrated strong predictive performance. The results  
257 of this study suggested that XGBMs, coupled with a SMOTE oversampling method, may be employed  
258 to successfully overcome the class imbalance problem and effectively predict complication outcomes in  
259 DBS surgery. This method may be used to estimate any individual patient's risk of complications.  
260 Plotting feature importance demonstrated that age, BMI, gender, procedure side, a diagnosis of  
261 Parkinson's disease, the operating institution and preoperative comorbidities were influential predictors  
262 of postoperative complications. The results of this study that suggested associations between  
263 preoperative risk factors and postoperative adverse outcomes are supported by previous research  
264 demonstrating that many of these same factors are significantly associated with complication outcomes  
265 in DBS surgery<sup>31,70,71</sup> and in other forms of neurosurgery<sup>18,23,24,72,73</sup>.

266 Surgeons often perceive patterns in their clinical practice. Machine learning algorithms seem to  
267 approximate well the intuition of the surgeon. Postoperative complications are likely to arise as a result  
268 of complex interactions between many risk factors<sup>74</sup>. While logistic regression has been deployed in  
269 the past to predict surgical outcomes<sup>18,24</sup>, other supervised learning algorithms, including XGBM, may  
270 be better suited to modeling these complex nonlinear relationships<sup>44,48,75</sup>.

271 This study has demonstrated one potential approach to addressing the class imbalance problem,  
272 which is a major issue in surgical risk stratification<sup>18,19,24,31</sup>. The approach employed here, applying  
273 SMOTE oversampling in conjunction with the XGBM supervised learning algorithm, produced  
274 encouraging results.

275 Simple linear relationships between risks and outcomes are intuitive. Linear and logistic regression  
276 generate statistical weights associated with each predictor and can be represented with a linear equation.  
277 These approaches offer rapid interpretability and an impression of understandability. In contrast,



278 advanced supervised machine learning algorithms are often more complex, inscrutable and opaque.  
279 Surgeons are likely to have a lower level of trust in, and therefore may demonstrate weaker adoption of,  
280 opaque machine learning algorithms as decision support tools. The XGBM performance statistics,  
281 feature importance plots and hypothetical cases generated help to address this issue by providing some  
282 insight into the mechanics of the XGBM models developed. More work on developing the  
283 “explainability” of these models is required.

284 A collection of hypothetical cases was presented to demonstrate the risk stratification outputs of the  
285 supervised learning models developed. There may be a tendency to attempt to identify patterns in the  
286 hypothetical patient data displayed and the corresponding risk evaluation output statistics. However,  
287 this tendency is fraught because the number of hypothetical cases displayed is small and the algorithms  
288 are able to model complex nonlinearities in the data, based on hundreds of training cases, which are  
289 likely to evade human judgement. Similar to previous research<sup>18</sup>, these examples provide a random  
290 selection of cases and patient characteristics to offer clinicians a general sense of the predictive risk  
291 outputs of the models trained. They are not intended to offer a systematic demonstration of the complex  
292 relationships modeled by the trained algorithms.

293 These machine learning models have the potential to facilitate patient safety improvements<sup>76</sup>. They  
294 may be used to stimulate a deeper conversation about complications with a patient prior to surgery,  
295 more attention throughout the process from the surgeon and surgical team, closer patient follow-up and  
296 activation of other organizational patient support processes postoperatively. Models of this nature  
297 should form part of a broader comprehensive approach to clinical risk stratification and patient safety  
298 improvement. As an example from another domain of neurosurgery, the Seattle Spine Team has  
299 developed a systematic and standardised approach that incorporates multidisciplinary patient review  
300 conferences, specialized clinical teams, intraoperative monitoring protocols and multi-surgeon  
301 operating practices, in addition to the development of experimental decision support systems  
302 underpinned by machine learning methods<sup>24,77-84</sup>.

303 The advantages of using machine learning methods to stratify risk in neurosurgery are numerous.  
304 Machine learning methods are more capable of capturing complex nonlinearities in very large datasets

305 than traditional statistical techniques and can be deployed to production using cloud computing services  
306 for potential use by clinicians and patients globally<sup>85,86</sup>. These tools are well-suited to high-volume  
307 complex data processing, they facilitate access to information, they save time and they have the  
308 potential to augment the clinical functioning of the neurosurgeon. Incorporating machine learning tools  
309 into the neurosurgical workflow may assist in reducing the likelihood of clinical error and positively  
310 engaging the patient. Supervised machine learning models can provide accurate and individualized  
311 outcome predictions, which are likely to be beneficial as healthcare progresses toward a future that is  
312 more precise and value based. Prediction datapoints may feed into and influence perioperative care  
313 processes and decisions or intraoperative treatment by human and robotic systems. On the other hand, it  
314 may not be suitable to apply machine learning methods to datasets that are erroneous, exceedingly  
315 noisy, obsolete or biased. In these cases, it may be preferable to rely on the unassisted judgment of the  
316 expert surgeon and an experienced clinical team.

### 317 **Limitations and future research**

318 The performance metrics using SMOTE oversampling and extreme gradient boosting were strong.  
319 Such high performance of the XGBM algorithms suggests that some degree of overfitting may have  
320 occurred, despite built-in overfitting mitigation. This, however, is difficult to assess, particularly in the  
321 context of limited case data. Caution and appropriate clinical judgement should be exercised if  
322 deploying and using these models to make predictions on new patient data. Further validation on new  
323 data from other institutions and larger datasets would be beneficial.

324 While assessing the effects of the use of intraoperative CT on complication rates and patient  
325 outcomes was beyond the scope of this study, it may have been beneficial to control for its use in the  
326 analysis. Per patient labelling of this variable was not captured in the dataset and this is therefore a  
327 limitation of this study. Similarly, it would be beneficial for future predictive modeling studies to  
328 control for additional preoperative clinical variables in multivariate analyses. These may include pre-  
329 and post-operative functional status, anemia, operating time, the number of electrode passes, passage  
330 through the ventricle and a patient history of coronary artery disease or stroke.

331 A primary aim of this study was to develop models capable of stratifying patient complication risk  
332 in DBS surgery. To achieve this and to mitigate the limitations of the dataset, complication  
333 subcategories were amalgamated into a superordinate variable representing general clinical risk and  
334 adverse outcomes. This approach allowed the development of a set of useful and applicable models.  
335 However, it must be noted that these models are broad in their risk predictions and that to predict  
336 specific types of complications, which would enable the implementation of specific clinical risk  
337 mitigation tactics (e.g., augmented infection prevention or operating room preparation for a returning  
338 patient), larger datasets and more modeling work are required. The variables included in the  
339 superordinate complication outcome variable fall logically under the banner of adverse postoperative  
340 clinical events. While the specific outcomes that make up this variable may be considered diverse,  
341 amalgamating them remains clinically useful because together they broadly indicate high risk patients  
342 that may require additional critical clinical thought and discussion, resources and careful perioperative  
343 management.

344 Future research may deploy the methods applied here for the prediction of complications associated  
345 with other surgical procedures that are characterized by a similar class imbalance problem. Studies may  
346 also develop supervised learning models to predict positive functional outcomes and the degree of  
347 functional improvement associated with various neurosurgical procedures. Future work may focus on  
348 the development of clinical decision support systems to be applied in clinical practice and to deliver  
349 decision-support benefits directly to patients via application to patient consultations in the clinics<sup>87</sup>.

## 350 **Conclusion**

351 Significant complication risk factors were detected and supervised machine learning algorithms  
352 effectively predicted adverse outcomes in DBS surgery. These supervised learning models can be used  
353 for the improvement of risk stratification, preoperative patient informed consent and clinical planning  
354 to make DBS surgery safer for patients. XGBMs and SMOTE appear to be useful tools for the  
355 prediction of complication outcomes and risk stratification in DBS surgical practice.

356

357 **REFERENCES**

- 358 1. Rumalla, K., Smith, K. A., Follett, K., Nazzaro, J. & Arnold, P. M. Rates, Causes, Risk Factors,  
359 and Outcomes of Readmission Following Deep Brain Stimulation for Movement Disorders:  
360 Analysis of the US Nationwide Readmissions Database. *Clin. Neurol. Neurosurg.* (2018).
- 361 2. Zhou, J. J., Chen, T., Farber, S. H., Shetter, A. G. & Ponce, F. A. Open-loop deep brain  
362 stimulation for the treatment of epilepsy: a systematic review of clinical outcomes over the past  
363 decade (2008–present). *Neurosurg. Focus* **45**, E5 (2018).
- 364 3. Matias, C. M., Frizon, L. A., Nagel, S. J., Lobel, D. A. & Machado, A. G. Deep brain  
365 stimulation outcomes in patients implanted under general anesthesia with frame-based  
366 stereotaxy and intraoperative MRI. *J. Neurosurg.* 1–7 (2018).
- 367 4. Kleiner-Fisman, G. *et al.* Subthalamic nucleus deep brain stimulation: summary and meta-  
368 analysis of outcomes. *Mov. Disord. Off. J. Mov. Disord. Soc.* **21**, S290–S304 (2006).
- 369 5. Mueller, J. *et al.* Pallidal deep brain stimulation improves quality of life in segmental and  
370 generalized dystonia: results from a prospective, randomized sham-controlled trial. *Mov.*  
371 *Disord.* **23**, 131–134 (2008).
- 372 6. Flora, E. Della, Perera, C. L., Cameron, A. L. & Maddern, G. J. Deep brain stimulation for  
373 essential tremor: a systematic review. *Mov. Disord.* **25**, 1550–1559 (2010).
- 374 7. Schrock, L. E. *et al.* Tourette syndrome deep brain stimulation: a review and updated  
375 recommendations. *Mov. Disord.* **30**, 448–471 (2015).
- 376 8. Herzog, J. *et al.* Most effective stimulation site in subthalamic deep brain stimulation for  
377 Parkinson’s disease. *Mov. Disord.* **19**, 1050–1054 (2004).
- 378 9. Odekerken, V. J. J. *et al.* Subthalamic nucleus versus globus pallidus bilateral deep brain  
379 stimulation for advanced Parkinson’s disease (NSTAPS study): a randomised controlled trial.  
380 *Lancet Neurol.* **12**, 37–44 (2013).
- 381 10. Schlaepfer, T. E., Bewernick, B. H., Kayser, S., Mädler, B. & Coenen, V. A. Rapid effects of

- 382 deep brain stimulation for treatment-resistant major depression. *Biol. Psychiatry* **73**, 1204–1212  
383 (2013).
- 384 11. Little, S. *et al.* Adaptive deep brain stimulation in advanced Parkinson disease. *Ann. Neurol.* **74**,  
385 449–457 (2013).
- 386 12. Miocinovic, S., Somayajula, S., Chitnis, S. & Vitek, J. L. History, applications, and mechanisms  
387 of deep brain stimulation. *JAMA Neurol.* **70**, 163–171 (2013).
- 388 13. Figeo, M. *et al.* Deep brain stimulation restores frontostriatal network activity in obsessive-  
389 compulsive disorder. *Nat. Neurosci.* **16**, 386–387 (2013).
- 390 14. Rodriguez-Oroz, M. C. *et al.* Bilateral deep brain stimulation in Parkinson's disease: a  
391 multicentre study with 4 years follow-up. *Brain* **128**, 2240–2249 (2005).
- 392 15. Kalakoti, P. *et al.* Predictors of unfavorable outcomes following deep brain stimulation for  
393 movement disorders and the effect of hospital case volume on outcomes: an analysis of 33, 642  
394 patients across 234 US hospitals using the National (Nationwide) Inpatient Sample from 20.  
395 *Neurosurg. Focus* **38**, E4 (2015).
- 396 16. Zrinzo, L., Foltynie, T., Limousin, P. & Hariz, M. I. Reducing hemorrhagic complications in  
397 functional neurosurgery: a large case series and systematic literature review. *J. Neurosurg.* **116**,  
398 84–94 (2012).
- 399 17. Hardaway, F. A., Raslan, A. M. & Burchiel, K. J. Deep brain stimulation-related infections:  
400 analysis of rates, timing, and seasonality. *Neurosurgery* **83**, 540–547 (2017).
- 401 18. Khor, S. *et al.* Development and validation of a prediction model for pain and functional  
402 outcomes after lumbar spine surgery. *JAMA Surg.* **153**, 634–642 (2018).
- 403 19. Buchlak, Q. D. *et al.* Machine learning applications to clinical decision support in neurosurgery:  
404 an artificial intelligence augmented systematic review. *Neurosurg. Rev.* 1–19 (2019).  
405 doi:<https://doi.org/10.1007/s10143-019-01163-8>
- 406 20. Senders, J. T. *et al.* Machine learning and neurosurgical outcome prediction: a systematic

- 407 review. *World Neurosurg.* **109**, 476–486 (2018).
- 408 21. Boachie-Adjei, O. *et al.* Surgical Risk Stratification Based on Preoperative Risk Factors in  
409 Severe Pediatric Spinal Deformity Surgery. *Spine Deform.* **2**, 340–349 (2014).
- 410 22. Bilimoria, K. Y. *et al.* Development and evaluation of the universal ACS NSQIP surgical risk  
411 calculator: a decision aid and informed consent tool for patients and surgeons. *J. Am. Coll. Surg.*  
412 **217**, 833-842. e3 (2013).
- 413 23. Bekelis, K., Desai, A., Bakhom, S. F. & Missios, S. A predictive model of complications after  
414 spine surgery: The National Surgical Quality Improvement Program (NSQIP) 2005-2010. *Spine*  
415 *J.* **14**, 1247–1255 (2014).
- 416 24. Buchlak, Q. D. *et al.* The Seattle spine score: Predicting 30-day complication risk in adult spinal  
417 deformity surgery. *J. Clin. Neurosci.* (2017). doi:10.1016/j.jocn.2017.06.012
- 418 25. Stopa, B. M., Yan, S. C., Dasenbrock, H. H., Kim, D. H. & Gormley, W. B. Variance reduction  
419 in neurosurgical practice: The case for analytics driven decision support in the era of Big Data.  
420 *World Neurosurg.* (2019).
- 421 26. Angeles, P., Tai, Y., Pavese, N., Wilson, S. & Vaidyanathan, R. Automated assessment of  
422 symptom severity changes during deep brain stimulation (DBS) therapy for Parkinson’s disease.  
423 in *2017 International Conference on Rehabilitation Robotics (ICORR)* 1512–1517 (IEEE,  
424 2017).
- 425 27. Kostoglou, K. *et al.* Classification and Prediction of Clinical Improvement in Deep Brain  
426 Stimulation From Intraoperative Microelectrode Recordings. *IEEE Trans. Biomed. Eng.* **64**,  
427 1123–1130 (2017).
- 428 28. Taghva, A. Hidden semi-Markov models in the computerized decoding of microelectrode  
429 recording data for deep brain stimulator placement. *World Neurosurg.* **75**, 758–763 (2011).
- 430 29. Taghva, A. An automated navigation system for deep brain stimulator placement using hidden  
431 Markov models. *Oper. Neurosurg.* **66**, ons-108 (2010).

- 432 30. Baumgarten, C. *et al.* Image-guided preoperative prediction of pyramidal tract side effect in  
433 deep brain stimulation: proof of concept and application to the pyramidal tract side effect  
434 induced by pallidal stimulation. *J. Med. Imaging* **3**, 25001 (2016).
- 435 31. Buchlak, Q. D., Kowalczyk, M., Leveque, J.-C., Wright, A. & Farrokhi, F. Risk stratification in  
436 deep brain stimulation surgery: Development of an algorithm to predict patient discharge  
437 disposition with 91.9% accuracy. *J. Clin. Neurosci.* (2018).
- 438 32. Wong, S., Baltuch, G. H., Jaggi, J. L. & Danish, S. F. Functional localization and visualization  
439 of the subthalamic nucleus from microelectrode recordings acquired during DBS surgery with  
440 unsupervised machine learning. *J. Neural Eng.* **6**, 26006 (2009).
- 441 33. Valsky, D. *et al.* Stop! border ahead: Automatic detection of subthalamic exit during deep brain  
442 stimulation surgery. *Mov. Disord.* **32**, 70–79 (2017).
- 443 34. Zaidel, A., Spivak, A., Shpigelman, L., Bergman, H. & Israel, Z. Delimiting subterritories of the  
444 human subthalamic nucleus by means of microelectrode recordings and a Hidden Markov  
445 Model. *Mov. Disord.* **24**, 1785–1793 (2009).
- 446 35. Zhang, Y. & Haghani, A. A gradient boosting method to improve travel time prediction. *Transp.*  
447 *Res. Part C Emerg. Technol.* **58**, 308–324 (2015).
- 448 36. Friedman, J. H. Greedy function approximation: a gradient boosting machine. *Ann. Stat.* 1189–  
449 1232 (2001).
- 450 37. Lu, J. *et al.* Estimation of elimination half-lives of organic chemicals in humans using gradient  
451 boosting machine. *Biochim. Biophys. Acta (BBA)-General Subj.* **1860**, 2664–2671 (2016).
- 452 38. Touzani, S., Granderson, J. & Fernandes, S. Gradient boosting machine for modeling the energy  
453 consumption of commercial buildings. *Energy Build.* **158**, 1533–1543 (2018).
- 454 39. Rawi, R. *et al.* PaRSnIP: sequence-based protein solubility prediction using gradient boosting  
455 machine. *Bioinformatics* **34**, 1092–1098 (2017).
- 456 40. Fan, J. *et al.* Comparison of Support Vector Machine and Extreme Gradient Boosting for

- 457 predicting daily global solar radiation using temperature and precipitation in humid subtropical  
458 climates: A case study in China. *Energy Convers. Manag.* **164**, 102–111 (2018).
- 459 41. Esmaili, N., Piccardi, M., Kruger, B. & Girosi, F. Analysis of healthcare service utilization after  
460 transport-related injuries by a mixture of hidden Markov models. *PLoS One* **13**, e0206274  
461 (2018).
- 462 42. Brown, I. & Mues, C. An experimental comparison of classification algorithms for imbalanced  
463 credit scoring data sets. *Expert Syst. Appl.* **39**, 3446–3453 (2012).
- 464 43. He, H. & Garcia, E. A. Learning from imbalanced data. *IEEE Trans. Knowl. Data Eng.* 1263–  
465 1284 (2008).
- 466 44. Raschka, S. & Mirjalili, V. *Python machine learning*. (Packt Publishing Ltd, 2017).
- 467 45. Grigsby, J., Kramer, R. E., Schneiders, J. L., Gates, J. R. & Brewster Smith, W. Predicting  
468 outcome of anterior temporal lobectomy using simulated neural networks. *Epilepsia* **39**, 61–66  
469 (1998).
- 470 46. Abouzari, M., Rashidi, A., Zandi-Toghiani, M., Behzadi, M. & Asadollahi, M. Chronic subdural  
471 hematoma outcome prediction using logistic regression and an artificial neural network.  
472 *Neurosurg. Rev.* (2009). doi:10.1007/s10143-009-0215-3
- 473 47. Patel, J. L. & Goyal, R. K. Applications of artificial neural networks in medical science. *Curr.*  
474 *Clin. Pharmacol.* **2**, 217–226 (2007).
- 475 48. Kim, J. S. *et al.* Predicting Surgical Complications in Patients Undergoing Elective Adult Spinal  
476 Deformity Procedures Using Machine Learning. *Spine Deform.* **6**, 762–770 (2018).
- 477 49. Japkowicz, N. & Stephen, S. The class imbalance problem: A systematic study. *Intell. data*  
478 *Anal.* **6**, 429–449 (2002).
- 479 50. Chawla, N. V. Data mining for imbalanced datasets: An overview. in *Data mining and*  
480 *knowledge discovery handbook* 875–886 (Springer, 2009).
- 481 51. Japkowicz, N. The class imbalance problem: Significance and strategies. in *Proc. of the Int'l*



- 482 *Conf. on Artificial Intelligence* (2000).
- 483 52. Mazurowski, M. A. *et al.* Training neural network classifiers for medical decision making: The  
484 effects of imbalanced datasets on classification performance. *Neural networks* **21**, 427–436  
485 (2008).
- 486 53. Kotsiantis, S., Kanellopoulos, D. & Pintelas, P. Handling imbalanced datasets: A review.  
487 *GESTS Int. Trans. Comput. Sci. Eng.* **30**, 25–36 (2006).
- 488 54. Sahin, Y., Bulkan, S. & Duman, E. A cost-sensitive decision tree approach for fraud detection.  
489 *Expert Syst. Appl.* **40**, 5916–5923 (2013).
- 490 55. Japkowicz, N., Myers, C. & Gluck, M. A novelty detection approach to classification. in *IJCAI*  
491 **1**, 518–523 (1995).
- 492 56. Kubat, M., Holte, R. C. & Matwin, S. Machine learning for the detection of oil spills in satellite  
493 radar images. *Mach. Learn.* **30**, 195–215 (1998).
- 494 57. Liu, X.-Y., Wu, J. & Zhou, Z.-H. Exploratory undersampling for class-imbalance learning. *IEEE*  
495 *Trans. Syst. Man, Cybern. Part B* **39**, 539–550 (2008).
- 496 58. Seiffert, C., Khoshgoftaar, T. M., Van Hulse, J. & Napolitano, A. RUSBoost: A hybrid approach  
497 to alleviating class imbalance. *IEEE Trans. Syst. Man, Cybern. A Syst. Humans* **40**, 185–197  
498 (2009).
- 499 59. Chawla, N. V., Bowyer, K. W., Hall, L. O. & Kegelmeyer, W. P. SMOTE: synthetic minority  
500 over-sampling technique. *J. Artif. Intell. Res.* **16**, 321–357 (2002).
- 501 60. Carlson, J. D., McLeod, K. E., McLeod, P. S. & Mark, J. B. Stereotactic accuracy and surgical  
502 utility of the O-arm in deep brain stimulation surgery. *Oper. Neurosurg.* **13**, 96–107 (2016).
- 503 61. Sterne, J. A. C. *et al.* Multiple imputation for missing data in epidemiological and clinical  
504 research: potential and pitfalls. *Bmj* **338**, b2393 (2009).
- 505 62. Raghunathan, T. E., Lepkowski, J. M., Van Hoewyk, J. & Solenberger, P. A multivariate  
506 technique for multiply imputing missing values using a sequence of regression models. *Surv.*

- 507 *Methodol.* **27**, 85–96 (2001).
- 508 63. Horton, N. J. & Kleinman, K. P. Much ado about nothing: A comparison of missing data  
509 methods and software to fit incomplete data regression models. *Am. Stat.* **61**, 79–90 (2007).
- 510 64. Steyerberg, E. W. & van Veen, M. Imputation is beneficial for handling missing data in  
511 predictive models. *J. Clin. Epidemiol.* **60**, 979 (2007).
- 512 65. Batista, G. E. & Monard, M. C. An analysis of four missing data treatment methods for  
513 supervised learning. *Appl. Artif. Intell.* **17**, 519–533 (2003).
- 514 66. Chen, T. & Guestrin, C. Xgboost: A scalable tree boosting system. in *Proceedings of the 22nd*  
515 *acm sigkdd international conference on knowledge discovery and data mining* 785–794 (ACM,  
516 2016).
- 517 67. Senders, J. T. *et al.* Natural and artificial intelligence in neurosurgery: a systematic review.  
518 *Neurosurgery* (2017).
- 519 68. Saad, F. & Mansinghka, V. Probabilistic Data Analysis with Probabilistic Programming. 1–46  
520 (2016).
- 521 69. Gabb, G. M. *et al.* Guideline for the diagnosis and management of hypertension in adults—  
522 2016. *Med. J. Aust.* **205**, 85–89 (2016).
- 523 70. Hu, K., Moses, Z. B., Hutter, M. M. & Williams, Z. Short-term adverse outcomes after deep  
524 brain stimulation treatment in patients with parkinson disease. *World Neurosurg.* **98**, 365–374  
525 (2017).
- 526 71. Tanaka, M. *et al.* Risk Factors for Postoperative Delirium After Deep Brain Stimulation Surgery  
527 for Parkinson Disease. *World Neurosurg.* **114**, e518–e523 (2018).
- 528 72. Akins, P. T. *et al.* Risk factors associated with 30-day readmissions after instrumented spine  
529 surgery in 14,939 patients. *Spine (Phila. Pa. 1976)*. **40**, 1022–1032 (2015).
- 530 73. Murphy, M. E. *et al.* Predictors of Discharge to a Nonhome Facility in Patients Undergoing  
531 Lumbar Decompression Without Fusion for Degenerative Spine Disease. *Neurosurgery* (2017).

- 532 74. Cooney, M. T., Dudina, A. L. & Graham, I. M. Value and limitations of existing scores for the  
533 assessment of cardiovascular risk: a review for clinicians. *J. Am. Coll. Cardiol.* **54**, 1209–1227  
534 (2009).
- 535 75. Shi, H.-Y., Hwang, S.-L., Lee, K.-T. & Lin, C.-L. In-hospital mortality after traumatic brain  
536 injury surgery: a nationwide population-based comparison of mortality predictors used in  
537 artificial neural network and logistic regression models. *J. Neurosurg.* **118**, 746–752 (2013).
- 538 76. Bates, D. W. & Gawande, A. A. Improving safety with information technology. *N. Engl. J. Med.*  
539 **348**, 2526–2534 (2003).
- 540 77. Buchlak, Q. D., Yanamadala, V., Leveque, J.-C. & Sethi, R. Complication avoidance with pre-  
541 operative screening: insights from the Seattle spine team. *Curr. Rev. Musculoskelet. Med.* **9**,  
542 (2016).
- 543 78. Sethi, R. K. *et al.* The Seattle Spine Team approach to adult deformity surgery: a systems-based  
544 approach to perioperative care and subsequent reduction in perioperative complication rates.  
545 *Spine Deform.* **2**, 95–103 (2014).
- 546 79. Sethi, R. *et al.* A systematic multidisciplinary initiative for reducing the risk of complications in  
547 adult scoliosis surgery. *J. Neurosurg. Spine* **26**, (2017).
- 548 80. Sethi, R. K., Buchlak, Q. D., Leveque, J.-C., Wright, A. K. & Yanamadala, V. V. Quality and  
549 safety improvement initiatives in complex spine surgery. in *Seminars in Spine Surgery* **30**, 111–  
550 120 (Elsevier, 2018).
- 551 81. Yanamadala, V. *et al.* Multidisciplinary Evaluation Leads to the Decreased Utilization of  
552 Lumbar Spine Fusion. *Spine (Phila. Pa. 1976)*. **42**, (2017).
- 553 82. Bauer, J. M., Yanamadala, V., Shah, S. A. & Sethi, R. K. Two Surgeon Approach for Complex  
554 Spine Surgery: Rationale, Outcome, Expectations, and the Case for Payment Reform. *JAAOS-*  
555 *Journal Am. Acad. Orthop. Surg.* **27**, e408–e413 (2019).
- 556 83. Buchlak, Q. D., Yanamadala, V., Leveque, J.-C. & Sethi, R. Preoperative Clinical Evaluation of

- 557           Adult Lumbar Scoliosis. in *Adult Lumbar Scoliosis* 61–70 (Springer, 2017).
- 558   84.   Yanamadala, V., Buchlak, Q., Leveque, J. C. & Sethi, R. How to Decrease Complications in the  
559           Management of Adult Lumbar Scoliosis. *Instr. Course Lect.* **66**, 379–390 (2017).
- 560   85.   Dalbhanjan, P. Overview of deployment options on AWS. *Amaz. Whitepapers* (2015).
- 561   86.   Copeland, M., Soh, J., Puca, A., Manning, M. & Gollob, D. Microsoft azure and cloud  
562           computing. in *Microsoft Azure* 3–26 (Springer, 2015).
- 563   87.   Kawamoto, K., Houlihan, C. A., Balas, E. A. & Lobach, D. F. Improving clinical practice using  
564           clinical decision support systems: a systematic review of trials to identify features critical to  
565           success. *Bmj* **330**, 765 (2005).

**Figure legend:**

- *Figure 1: Schematic outline of the two main phases of the analysis process.*
- *Figure 2: ROC curves for each of the SMOTE XGBM models, derived from the holdout test validation datasets.*
- *Figure 3: Feature importance plots for each of the SMOTE XGBM models. BMI = body mass index. DM = diabetes mellitus. GPi = globus pallidus. HB = hemiballismus. HTN = hypertension. L = left. PD = Parkinson's Disease. R = right. STN = subthalamic nucleus. VIM = ventral intermedius nucleus.*
- *Figure 4: Joint plots of complicated cases (any complication; A) and uncomplicated cases (B) in our sample according to age and BMI. Complicated cases clustered at approximately age=70 and BMI=24, whereas uncomplicated cases clustered at approximately age=69 and BMI=28. Histograms plot age and BMI frequency distributions.*

Feature Category	Feature	Feature class	Count (%)
Predictors	Institution	Institution 1	201 (40%)
		Institution 2	300 (60%)
	Age	75 and over	70 (14%)
		Under 75	431 (86%)
	Gender	Male	318 (63%)
		Female	183 (37%)
	Diagnoses	Parkinson's disease	349 (70%)
		Essential tremor	129 (26%)
		Dystonia	11 (2%)
		Other	12 (2%)
	BMI	≥25	335 (67%)
		18 to 24.9	157 (31%)
		<18	9 (2%)
	Comorbidities and risk factors	Smoking history	25 (5%)
		Immune suppressed	25 (5%)
		Diabetes	67 (13%)
		Hypertension	231 (46%)
Procedure type	Subthalamic (STN)	349 (70%)	
	Thalamic (VIM)	128 (26%)	
	Globus pallidus internus (GPi)	22 (4%)	
	Other	2 (0%)	
Outcomes	Intracranial hemorrhage	15 (3%)	
	Readmission	17 (3%)	
	Ischemic infarction	3 (1%)	
	Seizure	3 (1%)	
	Lead fractures	18 (4%)	
	Electrode migration	8 (2%)	
	Battery loose or flipping	7 (1%)	
	Device malfunction	26 (5%)	
	Return to operating room	53 (11%)	
	Infection	27 (5%)	
	Hemiparesis	5 (1%)	
	Facial droop	6 (1%)	
	Sensory change	4 (1%)	
	Complication other	8 (2%)	
	Complication any	83 (17%)	
	Complication within 12 months	59 (12%)	

*Table 1: Descriptive statistics displaying the classes of each of the predictors and outcome features in the dataset of 501 DBS patients. Other diagnoses included cluster headache, Holmes tremor and Tourette Syndrome.*

		Any complication		Complication within 12 months		Return to the operating room		Infection	
		Coefficient	OR (95% CI)	Coefficient	OR (95% CI)	Coefficient	OR (95% CI)	Coefficient	OR (95% CI)
<b>Intercept</b>		0.35	1.55 (0.35, 6.90)	-0.60	0.55 (0.10, 3.00)	-0.79	0.46 (0.08, 2.67)	-2.20	0.11 (0.01, 1.11)
<b>Demographics</b>	Institution 02	<b>-0.82**</b>	<b>0.44</b> <b>(0.25, 0.78)</b>	<b>-1.03**</b>	<b>0.36</b> <b>(0.18, 0.70)</b>	-0.39	0.68 (0.35, 1.34)	--	--
	Age 75 and over	0.44	1.55 (0.77, 3.13)	0.53	1.70 (0.75, 3.84)	0.17	1.18 (0.50, 2.80)	0.90	2.45 (0.88, 6.78)
	Male	-0.09	0.91 (0.55, 1.51)	0.06	1.06 (0.58, 1.91)	-0.09	0.91 (0.50, 1.68)	0.13	1.14 (0.48, 2.68)
	BMI at implant	<b>-0.07*</b>	<b>0.94</b> <b>(0.89, 0.99)</b>	-0.05	0.95 (0.90, 1.01)	-0.04	0.96 (0.90, 1.02)	-0.06	0.95 (0.87, 1.03)
<b>Clinical features</b>	Diabetes	<b>0.84*</b>	<b>2.33</b> <b>(1.18, 4.60)</b>	0.78	2.17 (0.98, 4.80)	<b>1.02**</b>	<b>2.78</b> <b>(1.31, 5.88)</b>	0.56	1.75 (0.58, 5.29)
	Hypertension	0.00	1.00 (0.58, 1.73)	0.21	1.23 (0.65, 2.32)	-0.18	0.84 (0.43, 1.60)	0.83	2.29 (0.99, 5.30)
	Smoking history	0.16	1.18 (0.40, 3.46)	0.38	1.46 (0.45, 4.79)	0.27	1.31 (0.41, 4.25)	<b>1.44*</b>	<b>4.20</b> <b>(1.21, 14.61)</b>
	Immunosuppression	0.14	1.15 (0.38, 3.55)	0.35	1.42 (0.43, 4.67)	-1.30	0.27 (0.03, 2.27)	--	--
	ET	0.02	1.02 (0.23, 4.55)	0.53	1.70 (0.43, 6.67)	-0.02	0.98 (0.19, 5.09)	-0.45	0.64 (0.07, 5.96)
	Dystonia	-1.02	0.36 (0.03, 4.12)	--	--	-0.53	0.59 (0.05, 7.25)	--	--
	Diagnosis other	-0.59	0.55 (0.07, 4.17)	--	--	--	--	--	--
	Thalamic (Vim)	-0.10	0.91 (0.21, 4.04)	-1.11	0.33 (0.08, 1.33)	0.37	1.44 (0.28, 7.55)	-0.47	0.62 (0.07, 5.84)
	Globus pallidus internus (GPI)	0.58	1.78 (0.46, 6.97)	0.20	1.22 (0.32, 4.70)	0.60	1.82 (0.39, 8.51)	0.10	1.10 (0.21, 5.70)
	Left sided procedure	0.20	1.23 (0.65, 2.32)	0.50	1.65 (0.80, 3.38)	-0.05	0.95 (0.44, 2.07)	0.25	1.29 (0.46, 3.62)
	Right sided procedure	-0.23	0.79 (0.34, 1.85)	0.19	1.20 (0.49, 2.98)	-0.52	0.59 (0.20, 1.75)	0.32	1.37 (0.41, 4.62)
<b>LLR p-value</b>		p=0.09		p<0.05		p=0.54		p=0.21	

Table 2: Multivariate logistic regression modelling results. These results are based on analysis of the original (non-SMOTE) dataset. CI = confidence interval. LLR = log likelihood ratio. OR = odds ratio. The reference categories were: female, Parkinson's Disease, age <75, institution 01, an operation conducted on both sides and an STN procedure. \* $p < 0.05$ , \*\* $p < 0.01$ .

		Institution 01	Institution 02
Number of cases		201	300
Demographics	Age (mean, SD)	62.12 (10.52)	66.28 (9.94)
	BMI (mean, SD)	27.71 (5.47)	27.17 (4.62)
	Female	41%	34%
Diagnosis	Parkinson's disease	68%	71%
	Essential tremor	24%	27%
	Dystonia	1%	3%
Clinical features	Smoking history	5%	5%
	Immune suppressed	9%	2%
	Diabetes mellitus	13%	13%
	Hypertension	70%	30%
Target	STN	69%	70%
	VIM	27%	24%
	GPi	3%	5%
Procedure side	Left	36%	25%
	Right	17%	8%
	Both	47%	67%
Complication outcomes	Any complication	22%	13%
	Complication at 12 months	18%	7%
	Return to the operating room	11%	10%
	Infection	6%	5%

*Table 3: A comparison of case characteristics between institutions, demonstrating a notable difference in the prevalence of patients with hypertension and immune suppression.*



Data	Original Dataset								SMOTE Dataset							
Model	Any complication	Complication at 12 months	Return to operating room	Infection	Any complication	Complication at 12 months	Return to operating room	Infection	Any complication	Complication at 12 months	Return to operating room	Infection	Any complication	Complication at 12 months	Return to operating room	Infection
Performance on validation holdout datasets																
Accuracy	0.66	0.86	0.88	0.95	0.85	0.91	0.88	0.97	0.85	0.91	0.88	0.97	0.85	0.91	0.88	0.97
AUC	0.58	0.69	0.57	0.68	0.94	0.96	0.97	0.99	0.94	0.96	0.97	0.99	0.94	0.96	0.97	0.99
Sensitivity	0.07	0.00	0.00	0.00	0.96	0.98	0.99	1.00	0.96	0.98	0.99	1.00	0.96	0.98	0.99	1.00
Specificity	0.81	0.88	0.91	0.95	0.78	0.85	0.80	0.93	0.78	0.85	0.80	0.93	0.78	0.85	0.80	0.93
PPV	0.08	0.00	0.00	0.00	0.75	0.85	0.77	0.93	0.75	0.85	0.77	0.93	0.75	0.85	0.77	0.93
Confusion matrices																
Predicted	Actual								Actual							
	+	-	+	-	+	-	+	-	+	-	+	-	+	-	+	-
+	2	23	0	18	0	13	0	8	99	33	120	21	108	32	134	10
-	29	97	3	130	5	133	0	143	4	115	3	122	1	128	0	141

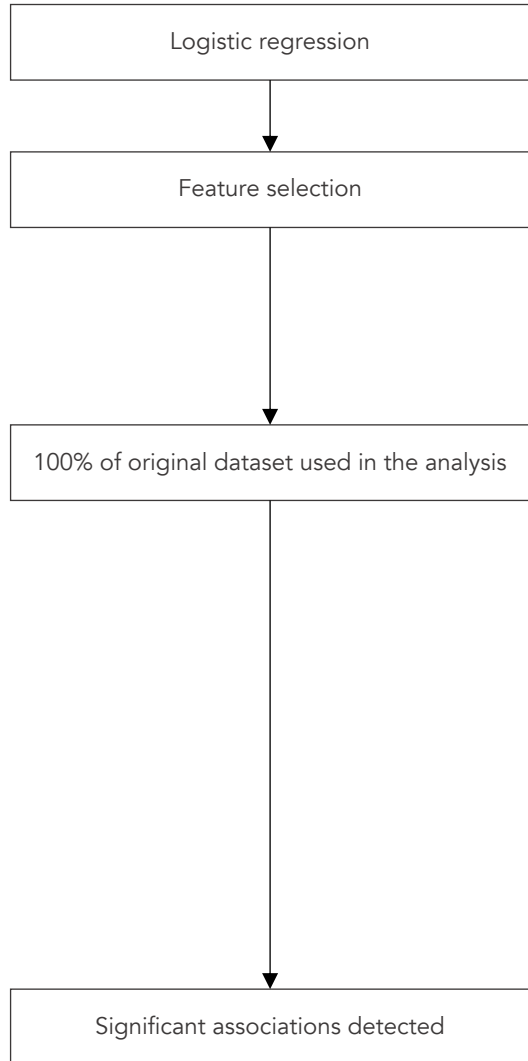
Table 4: Predictive performance metrics of XGBM models predicting (1) any complication, (2) complication within 12 months, (3) return to the operating room and (4) infection; using (a) the original dataset, and (b) the SMOTE oversampled training and validation datasets.

	Patient 1	Patient 2	Patient 3	Patient 4	Patient 5	Patient 6	Patient 7	Patient 8	Patient 9	Patient 10
Institution	1	1	1	1	2	2	2	2	1	2
Age at implant	33	48	63	75	33	48	54	78	57	76
Gender	F	F	M	M	M	M	F	F	M	M
BMI	18	24	30	27	28	35	22	29	35	40
Diagnosis	PD	Dyst	PD	PD	PD	ET	PD	PD	PD	ET
Smoking history	No	Yes	No	Yes	Yes	No	Yes	Yes	Yes	No
Immunosuppression	Normal	Normal	Normal	Yes	Normal	Normal	Yes	Normal	Yes	Normal
Diabetes status	--	DM	--	--	--	DM	--	DM	DM	DM
Hypertension status	--	--	HTN	--	HTN	--	--	HTN	HTN	--
Procedure target	STN	GPi	GPi	STN	STN	VIM	STN	STN	STN	VIM
Procedure side	Left	Both	Left	Right	Both	Both	Left	Both	Both	Right
Predicted probabilities of complication outcomes (likelihood shown in parentheses)										
Infection	M (11%)	H (25%)	L (7%)	H (29%)	H (17%)	L (4%)	M (10%)	M (12%)	H (16%)	H (19%)
Return to the operating room	M (12%)	VH (64%)	L (7%)	L (5%)	H (28%)	M (13%)	M (13%)	M (11%)	H (22%)	L (7%)
Any postoperative complication	H (43%)	VH (61%)	L (2%)	M (13%)	H (39%)	M (10%)	M (13%)	M (10%)	H (22%)	H (16%)
Postoperative complication within 12 months	M (14%)	H (19%)	L (2%)	H (32%)	L (6%)	L (8%)	H (17%)	L (3%)	H (23%)	H (31%)

*Table 5: Hypothetical patient characteristics and corresponding predicted complication likelihood. Risk thresholds are based on decision boundaries developed in cardiology: Low = <10%; Moderate = 10-15%; High = 16-50%; Very high = >50%. Dyst = dystonia. ET = essential tremor. GPi = globus pallidus. H = high. L = low. M = moderate. PD = Parkinson's Disease. STN = subthalamic nucleus. VH = very high. VIM = ventral intermedus nucleus.*

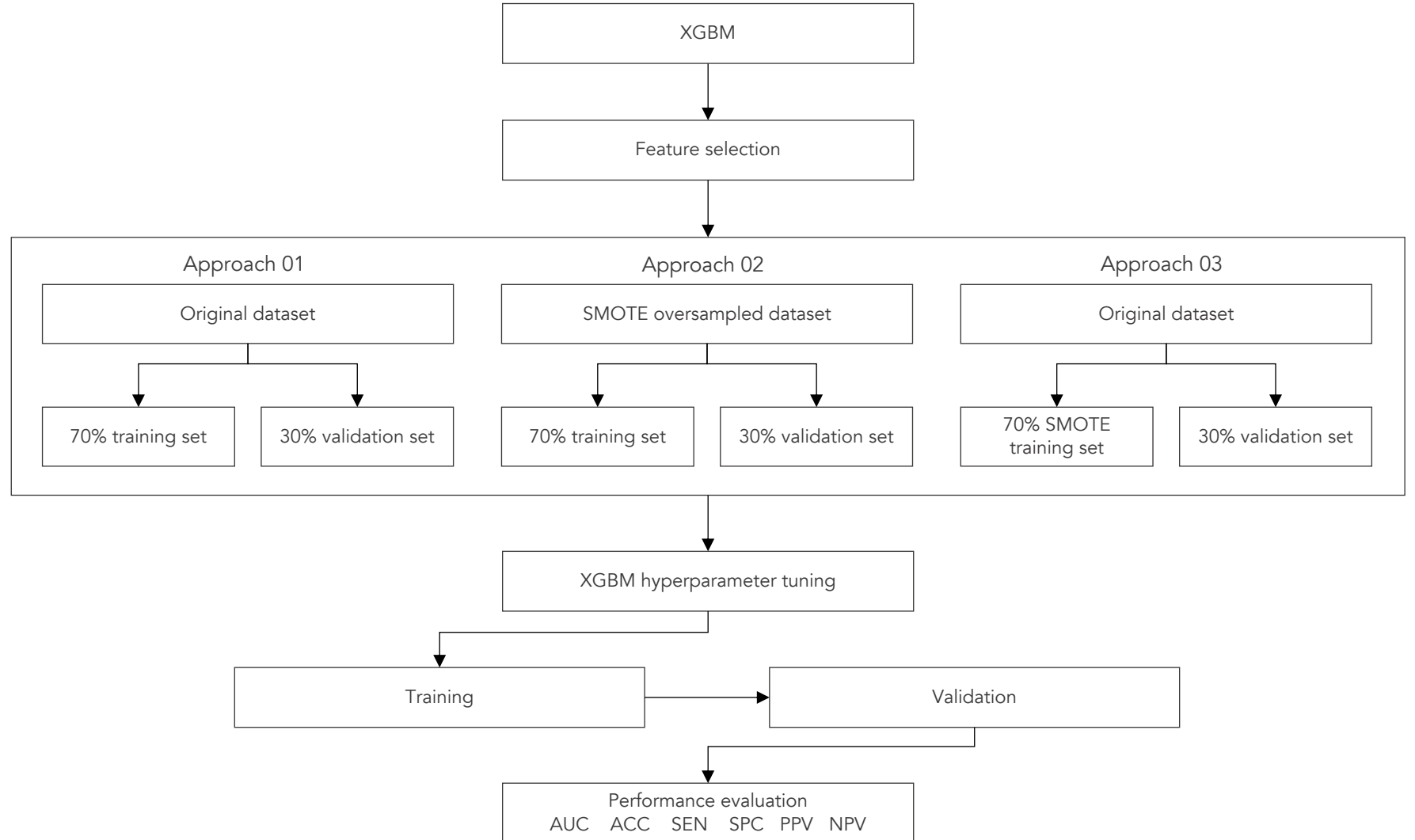
## Phase 1: Statistical Analysis

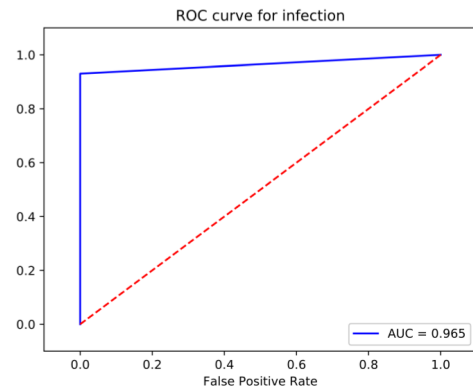
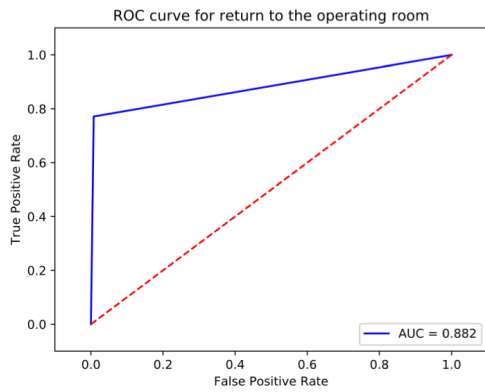
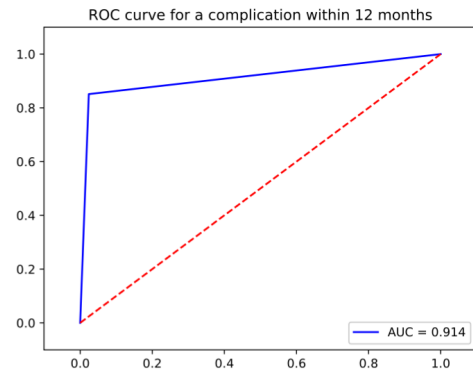
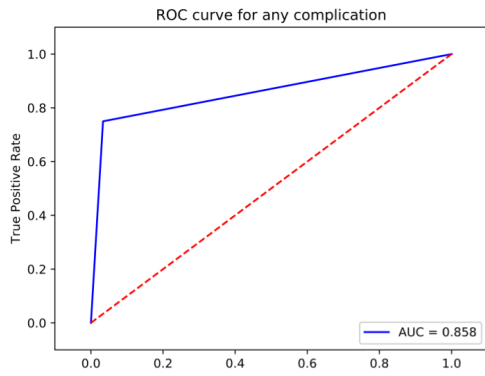
**Purpose:** Detect hypothesis-driven statistically significant associations



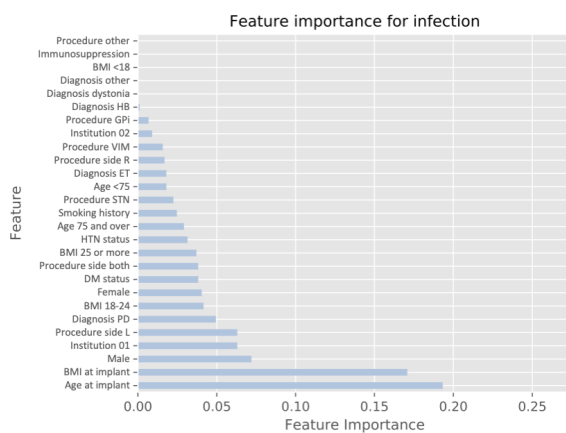
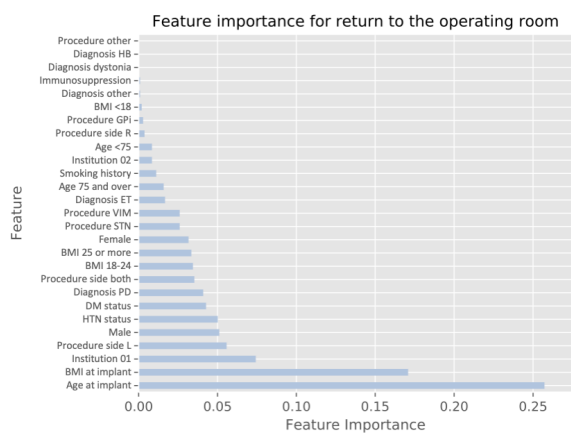
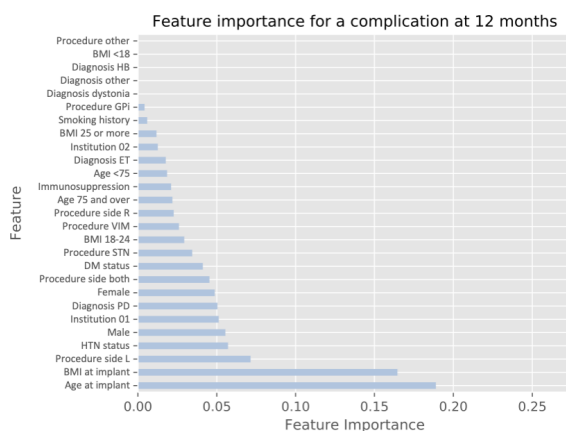
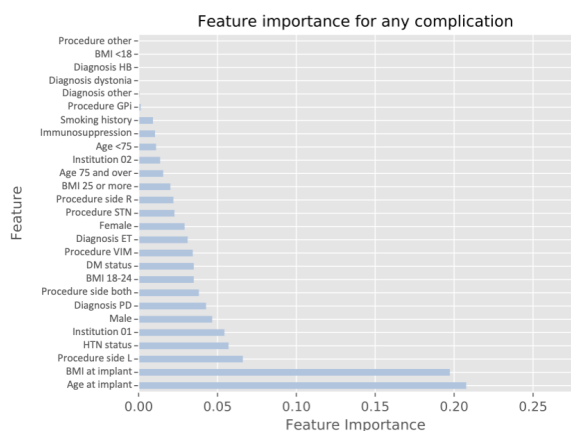
## Phase 2: Supervised Learning

**Purpose:** Train XGBM classifiers to enable complication prediction

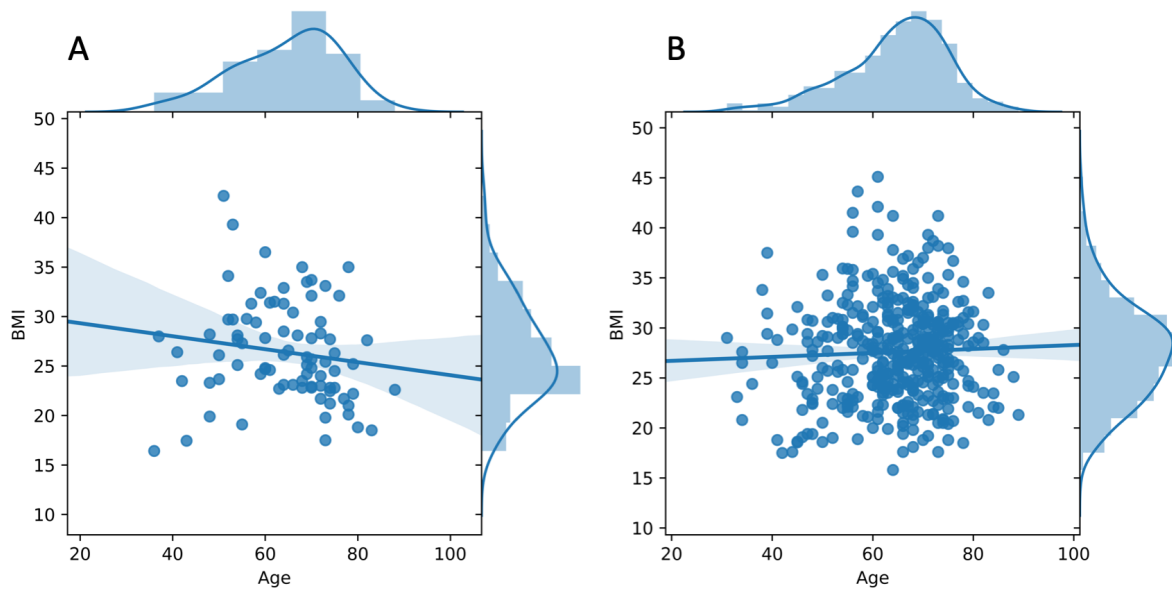




Journal



Journal



Journal Pre

## Abbreviations list

Abbreviation	Expansion / Meaning
AUC	area under the receiver operating characteristics curve
CI	confidence interval
DBS	deep brain stimulation
Dyst	dystonia
ET	essential tremor
GBM	gradient boosting machine
GPI	globus pallidus
H	High
L	Low
LLR	log likelihood ratio
M	Moderate
NPV	negative predictive value
OR	odds ratio
PD	Parkinson's disease
PPV	positive predictive value
ROC	receiver operating characteristics
SMOTE	Synthetic Minority Oversampling Technique
STN	subthalamic nucleus
VH	Very high
VIM	ventral intermedius nucleus
XGBM	extreme gradient boosting machine